

Managing Saline Water Intrusion in the Lower Indus Basin Aquifer

A. S. Chandio · T. S. Lee

Received: 26 May 2011 / Accepted: 22 December 2011 /
Published online: 17 January 2012
© Springer Science+Business Media B.V. 2012

Abstract In view of the declining surface water sources for irrigated agriculture in Pakistan, farmers are compelled to extract groundwater in order provide to security against uncertain canal supplies during critical crop growth periods. However saline water intrusion can be a major hindrance to the sustainable groundwater development. Against this background, a study was conducted with a three dimensional finite element model (FEMGWST) based on the Galerkin weighted residual method being developed to simulate groundwater flow and the saline water intrusion from underlying poor quality aquifer in response to groundwater pumping through low capacity partially penetrated wells. The model was calibrated with field data collected in the district Khairpur of the Lower Indus Basin. The stability of the model for transient groundwater flow and solute transport against different time marching schemes were evaluated. This study showed that the explicit and the Crank-Nicolson time marching schemes developed the numerical oscillating, the global error and the convergence problem. The calibrated model was applied to predict the impacts of different well configurations on the pumped water quality and on the development of saline water mound at the bottom of the well. It was observed that the saline water intrusion into the fresh groundwater layer was directly related to the well discharge, pumping time and inversely to the thickness of fresh-saline water interface and the number of well strainers installed. The model results suggested that intermittent pumping through multi strainer wells could effectively be used to suppress the saline water intrusion. However multi strainers wells were found to induce saline water intrusion when the thickness of fresh-saline water interface was reduced to 4 m.

Keywords 3-D Finite element model · Saline water intrusion · Indus Basin · Galerkin weighted method · Partially penetrated wells

1 Introduction

Irrigated agriculture in Pakistan is primarily practiced in the Indus Basin where the surface water supplies are limited and fluctuating throughout the year (Khan et al. 2008; Qureshi et al. 2008; Zardari and Cordery 2009). The rotational surface water allocation based on farm size instead of crop type and its growth stage is also a major hindrance to satisfy the agricultural demand (Zardari and Cordery 2009). This has led to farmers relying on the groundwater

A. S. Chandio (✉) · T. S. Lee
Department of Biological and Agricultural Engineering, Faculty of Engineering,
Universiti Putra Malaysia, Serdang, 43400 Selangor, DE, Malaysia
e-mail: chandioas3@yahoo.com

resources to meet the crop water requirements. The stress on groundwater resources increases with the decline in surface irrigation water supplies, especially during the crop sowing periods and canal closure times. In 1984 there were about 238 thousands tube wells in operation in Pakistan, but by 2004 the number of tube wells had increased to 931 thousands (Pakistan Agricultural Machinery Census 2004; Pakistan Water Economy Running Dry 2005). These wells are mostly located in fresh to marginal groundwater areas to supplement irrigation supplies but also act to intercept irrigation conveyance losses and the application losses.

Qureshi et al. (2010) pointed out that the growth of tubewells led to problems of groundwater depletion, degradation of groundwater quality, and well yield generally remains well below its potential levels. Rejani et al. (2008) pointed out that excessive groundwater pumping during non-monsoon seasons for rice cultivation had not only caused a significant decrease in groundwater levels but also induces seawater intrusion, in the area of the Balasore coastal groundwater basin in Orissa, India. Iglesias et al. (2007) reported that due to over pumping saline intrusion is a major concern to groundwater development in the Mediterranean region, to meet the high seasonal water demand, mainly for tourism development. Kourakos and Mantoglou (2010) reported that groundwater withdrawal causes seawater intrusion and degradation of water quality in the coastal aquifers of the island of Santorini. Similarly, groundwater depletion and saline water intrusion is a major concern to groundwater development in the Indus Basin, Pakistan (Ahmad et al. 2010; Ataie-Ashtiani and Ketabchi 2010; Chandio and Larock 1984; Khan et al. 2008; Iglesias et al. 2007; Qureshi et al. 2010; Saeed and Ashraf 2005; Saeed and Bruen 2004; Sufi et al. 1998).

In the Indus Basin, it had been established that a native saline water layer prevails below the fresh water zone. Hence a scientific approach is required to skim (tap) the fresh water without disturbing the underlying native saline water. Fresh and saline ground waters are miscible fluids with varying density and when they come into contact in a porous soil medium a fresh-saline water interface forms between them. When the overlying fresh water is pumped through a well, the fresh-saline water interface tends to deform and move vertically towards the bottom of the well. For as long as the pumping rate is below a critical discharge a stable saline mound develops at some depth below the bottom of the skimming well. As soon as, the pumping rate reaches the critical discharge, the cone becomes unstable and ruins the quality of fresh groundwater. Werner et al. (2009) conducted the laboratory experiment on salt water up-coning using a controlled sand tank model. They observed that after the apex of the plume is intercepted by the well, the salt plume start spreading horizontally. Khan et al. (2008) pointed out the degradation of aquifers is almost an irreversible process and needs special attention either to suppress the saline water intrusion process or stop it. The application of the saline groundwater for agricultural production will undoubtedly lead to the problems of soil salinity and sodicity.

It was realized that a gap exists in the knowledge of the groundwater modeling for the area of Lower Indus Basin aquifer. Previous researches were mostly conducted in the Central Indus Basin aquifer and based on the hydro geological conditions prevailing in the Chaj and Rachna Doab areas. Key variables such as anisotropy, heterogeneity, thickness of fresh groundwater, well penetration in fresh zone, the thickness of fresh groundwater cushion at the bottom of the well, the well pumping rate and well operation time were not properly addressed. These uncertainties are the reasons to initiate a guideline study for sustainable groundwater development at the Lower Indus Basin.

A three dimensional finite element (FEMGWST) model based on the Galerkin weighted residual methods was developed at Universiti Putra Malaysia to simulate groundwater flow and solute transport for the complex geo-hydro condition of the Lower Indus Basin aquifer system in Pakistan. The schematic outline of the fundamental processes used in the model development and its application is shown in Fig. 1 which illustrates the brief details of steps required for data collection, preparation of input data model, model development, model calibration and its application as a prediction tool.

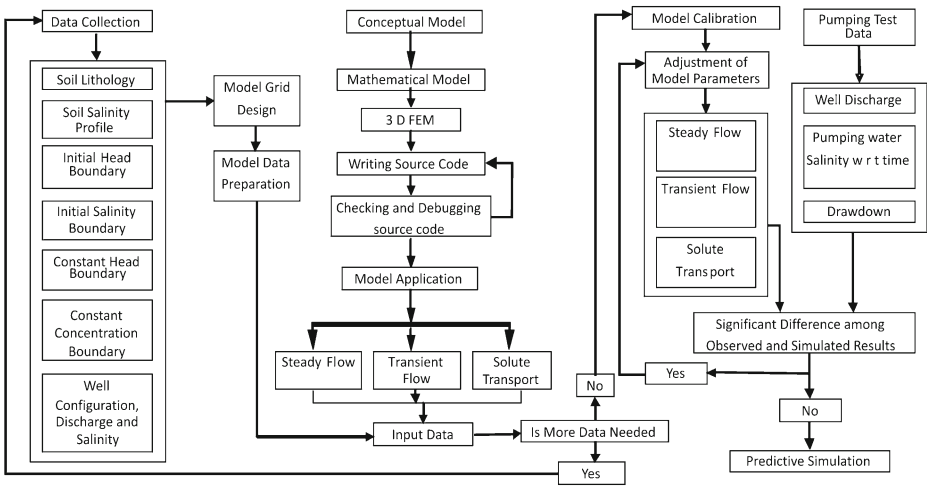


Fig. 1 Schematic outline for the development of 3-D finite element model and its application for groundwater flow and solute transport simulation

2 Description of Study Area

The study area covers about 10,000 ha that is bounded between the Rohri canal and the Khairpur Feeder East canal (KFE). The area is irrigated only by the KFE canal. The study area lies between latitudes 27°20'42" N and 27°19'23" N and longitudes 68°32'17" E and 68°35'57" E (Fig. 2). There is a great tendency to accumulate and store the groundwater seeping from the Indus River, conveyance losses from the irrigation network, and the field application losses in an unconfined aquifer. The aquifer consists of porous sandy material that is heterogeneous and anisotropic. During shortage of surface water supplies, water will be pumped through sixty nine shallow partially penetrated wells installed by farmers to meet crop water requirements. The design and installation of these skimming wells (composed of single or multi strainers) were not based on site specific knowledge of aquifer lithology and groundwater salinity profile but rather were based on water requirement and farmers' personal/community experiences, with mostly tubewell design options as provided by the local drillers (Saeed and Ashraf 2005). The diameters of single strainer wells vary between 10 and 30 cm while diameters of multi strainer well vary from 7.5 to 15 cm. The lengths of the skimming wells vary between 18 and 30 m. Due to the improper well design the consequence is either the pumping capacity reduces and/or water quality deteriorates within few months of installation. In the last 3 years, it was surveyed that about 31% of these farmers' tubewells were either abandoned or had their operations limited within the first 3 months after installation.

In this study, four tubewells installed at the Haroon agricultural farm (HTW), the Noor agricultural farm (NTW), the Karim agricultural farm (KTW) and the Sherdil agricultural farm (STW) were selected and a set of observation wells was installed to monitor the groundwater salinity and groundwater levels in response to pumping. The HTW is a double strainers (12 m apart from each other) skimming well, while the remaining wells (NTW, KTW and STW) are single strainer skimming wells. The detail configurations of these wells are shown in Table 1.

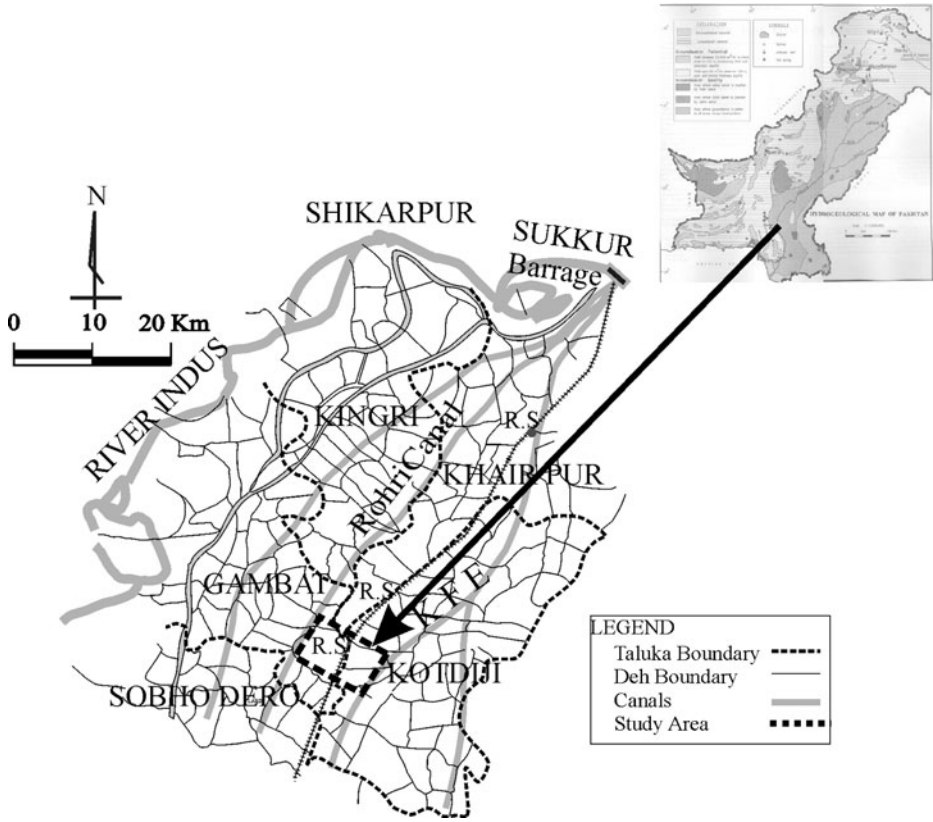


Fig. 2 Location of the study area in the lower Indus Basin, Pakistan

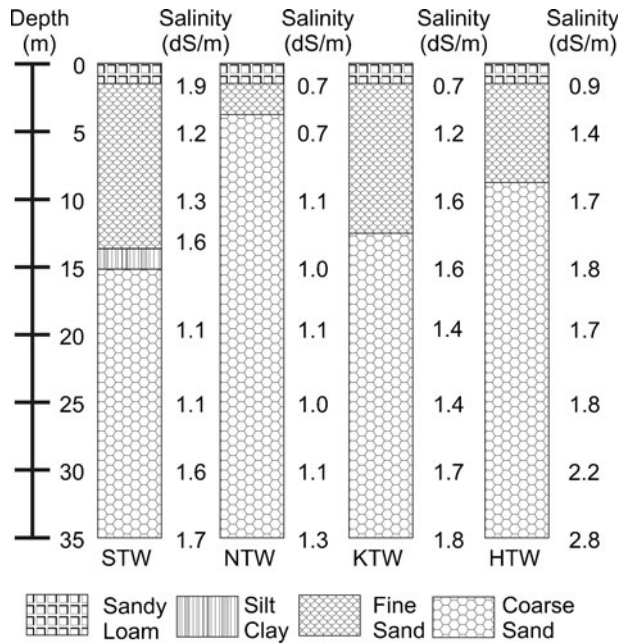
The soil lithology and groundwater salinity profiles at the site are shown in Fig. 3. The top layer is mostly classified as sandy loam while the rest of the profiles are fine sand and or predominantly coarse sand. The groundwater salinity profile up to 35 m depth was measured during test bores. However, unfortunately in the absence of new data the groundwater salinity profile for below 35 m had to be obtained from the old Lower Indus Project report (Hunting and MacDonald 1965). The salinity data of the profiles revealed that up to a 35 m depth the aquifer contains useable water with salinity that ranges between 600 and 1,214 parts per million (ppm), while beyond that depth salinity ranges between 1,568 and 3,000 ppm (Hunting and MacDonald 1965).

Table 1 Configurations of selected skimming wells in the study area

Tubewell configuration	HTW ¹	STW	KTW	NTW
Length of strainer (m)	10.70	16.80	12.20	20.00
Diesel Engine/E. Motor (Hp)	16.00	20.00	20.00	20.00 ²
Tubewell Discharge (liters/sec)	22.50 ³ 17.40 ⁴	26.30	27.00	31.20

Superscript 1 means pumping well (HTW) consists 2 bores, 2 means well is operated by Electric Motor, 3 means both bores of HTW are operated and 4 means one bore of HTW is in operation

Fig. 3 Soil lithology and salinity profile at the study area



3 Numerical Model Formulation

The three dimensional finite element model FEMGWST with a constant density approach, was developed to simulate the groundwater flow and solute transport for the study area only where sea water intrusion is not a problem and salinity up-coning occurs from the in-situ native saline layer. A constant density approach is said to be not appropriate for sea water intrusion (Bear and Verruijt 1990). The three dimensional movement of groundwater and salt concentration through unconfined aquifer may be described by the partial differential Eqs. 1 through 4.

$$\frac{\partial}{\partial x_\alpha} \left(K_{\alpha\beta} \frac{\partial h}{\partial x_\beta} \right) - Q = S_s \frac{\partial h}{\partial t} \tag{1}$$

$$\frac{\partial}{\partial x_\alpha} \left(D_{\alpha\beta} \frac{\partial C}{\partial x_\beta} - V_\alpha C \right) - QC = \frac{\partial C}{\partial t} \tag{2}$$

$$V_\alpha = - \left(\frac{K_{\alpha\beta}}{\eta} \right) \frac{\partial h}{\partial x_\beta} \tag{3}$$

$$D_{\alpha\beta} = a_T |V| \delta_{\alpha\beta} + \frac{(a_L - a_T) V_\alpha V_\beta}{|V|} \tag{4}$$

Where h is hydraulic head (L), K is hydraulic conductivity (LT^{-1}), x_α and x_β is Cartesian coordinates (L), t is time (T), Q is general source/sink term that defined the volume of inflow or outflow to the domain per unit volume of an aquifer (element) per unit time (T^{-1}), S_s is specific storativity of the aquifer (L^{-1}), C is solute concentration (ppm), $D_{\alpha\beta}$ is hydrodynamic dispersion coefficient (L^2T^{-1}), V_α is Cartesian component of velocity vector (LT^{-1}),

$|V|$ is average velocity (LT^{-1}), δ is Kronecker delta, α and β are subscripts represent x, y and z direction and η is porosity.

The Galerkin finite element method for space discretization proved to be robust for the simulation of groundwater flow and solute transport (Lenkopane et al. 2009). Thus the Galerkin weighted residual method was adopted to obtain the approximate solution for three dimensional groundwater flow so that Eq. 1 can be transformed as:

$$\int_{\Omega} \left(K_x \frac{\partial}{\partial x} \left(\frac{\partial \hat{h}}{\partial x} \right) + K_y \frac{\partial}{\partial y} \left(\frac{\partial \hat{h}}{\partial y} \right) + K_z \frac{\partial}{\partial z} \left(\frac{\partial \hat{h}}{\partial z} \right) - Q - S \frac{\partial \hat{h}}{\partial t} \right) N_i d\Omega = 0 \quad (5)$$

Where, N_i is a basis function and Ω represents the three dimensional domain.

The three-dimensional approximate trial solution of hydraulic head i.e. $\hat{h}(x, y, z)$ is expressed as a series of summation, and each term is the product of nodal head h_j , and nodal basis function $N_j(x, y, z)$, then:

$$\hat{h}(x, y, z) = \sum_{j=1}^{node} h_j N_j(x, y, z) \quad (6)$$

Substituting values of head into Eq. 5, it becomes a second order partial differential equation:

$$\int_{\Omega} \left(K_x \frac{\partial}{\partial x} \left(\frac{\partial h_j N_j}{\partial x} \right) + K_y \frac{\partial}{\partial y} \left(\frac{\partial h_j N_j}{\partial y} \right) + K_z \frac{\partial}{\partial z} \left(\frac{\partial h_j N_j}{\partial z} \right) - Q - S_s \frac{\partial (\partial h_j N_j)}{\partial t} \right) N_i d\Omega = 0 \quad (7)$$

Since, the solution of a second order partial differential equation could not be obtained directly hence, it is converted into a first order partial differential equation and then into a linear equation. Applying Green’s theorem, the second order partial differential equation is reduced to first order partial differential equation. Hence the first part of the Eq. 7 will yield to:

$$\int_{\Omega} K_x \frac{\partial}{\partial x} \left(\frac{\partial h_j}{\partial x} \right) N_j = \int_{\Gamma} N_j K_x \frac{\partial h_j}{\partial x} \ell_x d\Gamma - \int_{\Omega} h_j \left(K_x \frac{\partial N_i}{\partial x} \frac{\partial N_j}{\partial x} \right) d\Omega \quad (8)$$

$$\int_{\Omega} \left(S_s \frac{\partial (\partial h_j N_j)}{\partial t} \right) N_i d\Omega = \iiint_{\Omega} \left\{ \begin{matrix} N_1 \\ \vdots \\ N_8 \end{matrix} \right\} [S_s] \frac{\partial h}{\partial t} d\xi d\eta d\zeta \quad (9)$$

Bear and Cheng (2010), Chandio and Larock (1984) and Yu (1992) discussed in detail the representation of the pumping well. They presented the well as a one dimensional rod element and assumed that well discharge is distributed uniformly over the length of the element. Mathematically and physically the skimming well can easily be combined with any side of hexahedron element with concentrated flow at two nodes. Thus, in the groundwater modeling system the source or sink is directly computed and added to final global matrix. Considering Eq. 7, the source/sink term numerically may be defined as:

$$\iiint_{\Omega} N_i Q d\Omega = \sum_{k=1}^8 Q_k \left\{ \begin{matrix} N_1(x_k, y_k, z_k) \\ \vdots \\ N_8(x_k, y_k, z_k) \end{matrix} \right\} = \left\{ \begin{matrix} Q_1 \\ \vdots \\ Q_8 \end{matrix} \right\} \quad (10)$$

Where, Q_k is the discharge or recharge at the node k of an element. Since, k node may be connected to many elements, thus the element contained pumping or recharge well is assigned the value of Q_k while the remaining elements connected to the same node k must not be specified with Q_k . $d\Omega = d\xi d\eta d\zeta$ are the integrals over the entire domain. The Eq. 1 may be defined as:

$$\int_{\Omega} L(\widehat{h}) N_i d\Omega = \int_{-1}^1 \int_{-1}^1 \int_{-1}^1 \sum_{j=1}^8 \left[h_j \left(K_{\alpha\beta} \frac{\partial N_i}{\partial x_{\alpha}} \frac{\partial N_j}{\partial x_{\beta}} \right) + Q N_i + S_s \frac{d\widehat{h}}{dt} N_i \right] |J| d\xi d\eta d\zeta \tag{11}$$

$$- \int_{\Gamma} \left[K_{\alpha\beta} \frac{\partial \widehat{h}}{\partial \alpha} \ell_{\alpha} \right] N_i d\Gamma$$

$$\int_{-1}^1 \int_{-1}^1 \int_{-1}^1 \sum_{j=1}^8 \left(S_s \frac{d\widehat{h}}{dt} N_i \right) |J| d\xi d\eta d\zeta = \int_{-1}^1 \int_{-1}^1 \int_{-1}^1 \sum_{j=1}^8 \left(S_s \frac{\Delta h_j}{\Delta t} N_i N_j \right) |J| d\xi d\eta d\zeta \tag{12}$$

Following the above development, Eq. 7 may further be simplified into the following terms:

$$[A1_{ij}] = \int_{-1}^1 \int_{-1}^1 \int_{-1}^1 \sum_{j=1}^8 \frac{S_s}{\Delta t} N_i N_j |J| d\xi d\eta d\zeta \tag{13}$$

$$[A2_{ij}] = \int_{-1}^1 \int_{-1}^1 \int_{-1}^1 \sum_{j=1}^8 K_{\alpha\beta} \frac{\partial N_i}{\partial x_{\alpha}} \frac{\partial N_j}{\partial x_{\beta}} |J| d\xi d\eta d\zeta$$

$$\{A3_i\} = \int_{-1}^1 \int_{-1}^1 \int_{-1}^1 \sum_{j=1}^8 Q N_i |J| d\xi d\eta d\zeta \tag{14}$$

$$\{A4_i\} = \int_{\Gamma} \left[K_{\alpha\beta} \frac{\partial \widehat{h}}{\partial \alpha} \ell_{\alpha} \right] N_i d\Gamma = \int_{\Gamma} q_n N_i d\Gamma \tag{15}$$

Where q_n is the outward normal source flux (LT^{-1}), ℓ_{α} are the directional cosines in x , y and z direction. This boundary (Neumann Boundary) condition is valid when normal fluxes are specified; otherwise it is zero, as in case of the constant head boundaries (Dirichlet boundary). Finally, Eq. 7 takes the shape as:

$$[A1_{ij}] \{\Delta h_j\} + [A2_{ij}] \{h_j\} + \{A3_i\} - \{A4_i\} = 0 \tag{16}$$

For the transient groundwater flow, the head at the location of node j for the incremental time of $t + \Delta t$ may be calculated from Eq. 16 as:

$$([A1_{ij}] + \theta[A2_{ij}]) h_j^{t+\Delta t} = ([A1_{ij}] - (1 - \theta)[A2_{ij}]) h_j^{\Delta t} - \{A3_i\} + \{A4_i\} \tag{17}$$

The value of θ describes the time marching schemes.

Similarly, Eq. 2 may be written as:

$$\int_{\Omega} L(\widehat{C}) N_i d \Omega = \int_{\Omega} \left[\frac{\partial \widehat{C}}{\partial t} N_i + Q C_P N_i + \frac{\partial}{\partial x_{\alpha}} \left(\widehat{C} V_{\alpha} \right) N_i - \frac{\partial}{\partial x_{\alpha}} \left(D_{\alpha \beta} \frac{\partial \widehat{C}}{\partial x_{\beta}} \right) N_i \right] d \Omega \tag{18}$$

The rate of change in concentration may be expressed as:

$$\frac{\partial \widehat{C}}{\partial t} N_i d \Omega = \frac{1}{\Delta t} \int_{-1}^1 \int_{-1}^1 \int_{-1}^1 \sum_{j=1}^8 N_i N_j (C_j(t + \Delta t) - C_j(t)) |J| d \xi d \eta d \zeta \tag{19}$$

The sink term for the salts may be expressed as:

$$\int_{\Omega} Q C_P N_i d \Omega = \int_{\Omega} Q \widehat{C} N_i d \Omega \tag{20}$$

The convection dispersion term is decomposed into two parts as:

$$\int_{\Omega} \frac{\partial}{\partial x_{\alpha}} \left(\widehat{C} V_{\alpha} \right) N_i d \Omega = \int_{\Omega} \left(V_{\alpha} \frac{\partial \widehat{C}}{\partial x_{\alpha}} - Q \widehat{C} - S_S \frac{\partial \widehat{h}}{\partial t} \widehat{C} \right) N_i d \Omega \tag{21}$$

The solution of the convection dispersion term (Eq. 13) is also based on the values of the velocity tensor that had been already calculated in the process of solving the groundwater flow equations. The ultimate expression for the dispersion term can be ultimately written as:

$$\begin{aligned} \int_{\Omega} \frac{\partial}{\partial x_{\alpha}} \left(D_{\alpha \beta} \frac{\partial \widehat{C}}{\partial x_{\beta}} \right) = & \int_{-1}^1 \int_{-1}^1 \int_{-1}^1 \sum_j \left[C_j D_{\alpha \beta} \frac{\partial N_i}{\partial x_{\alpha}} \frac{\partial N_j}{\partial x_{\beta}} \right] |J| d \xi d \eta d \zeta \\ & - \int_{\Gamma} \left[D_{xx} \frac{\partial \widehat{C}}{\partial x} \ell_x + D_{yy} \frac{\partial \widehat{C}}{\partial y} \ell_y + D_{xy} \left(\frac{\partial \widehat{C}}{\partial y} \ell_x + \frac{\partial \widehat{C}}{\partial x} \ell_y \right) \right. \\ & \left. + D_{xz} \left(\frac{\partial \widehat{C}}{\partial z} \ell_x + \frac{\partial \widehat{C}}{\partial x} \ell_z \right) + D_{yz} \left(\frac{\partial \widehat{C}}{\partial z} \ell_y + \frac{\partial \widehat{C}}{\partial y} \ell_z \right) + D_{zz} \frac{\partial \widehat{C}}{\partial z} \ell_z \right] N_i d \Gamma \end{aligned} \tag{22}$$

Eqs. 19 to 22 can be described respectively in simpler terms as:

$$[B1_{ij}] = \sum_e \int_{-1}^1 \int_{-1}^1 \int_{-1}^1 \left[V_x \frac{\partial N_j}{\partial x} + V_y \frac{\partial N_j}{\partial y} + V_z \frac{\partial N_j}{\partial z} - S_S \frac{\partial \widehat{h}}{\partial t} \right] N_i |J| d \xi d \eta d \zeta \tag{23}$$

$$[B2_{ij}] = \sum_e \int_{-1}^1 \int_{-1}^1 \int_{-1}^1 \left(D_{\alpha \beta} \frac{\partial N_i}{\partial x_{\alpha}} \frac{\partial N_j}{\partial x_{\beta}} \right) |J| d \xi d \eta d \zeta \tag{24}$$

$$\begin{aligned} [B3_i] = & \int_{\Gamma} \left[D_{xx} \frac{\partial \widehat{C}}{\partial x} \ell_x + D_{yy} \frac{\partial \widehat{C}}{\partial y} \ell_y + D_{zz} \frac{\partial \widehat{C}}{\partial z} \ell_z + D_{xy} \left(\frac{\partial \widehat{C}}{\partial y} \ell_x + \frac{\partial \widehat{C}}{\partial x} \ell_y \right) \right. \\ & \left. + D_{xz} \left(\frac{\partial \widehat{C}}{\partial z} \ell_x + \frac{\partial \widehat{C}}{\partial x} \ell_z \right) + D_{yz} \left(\frac{\partial \widehat{C}}{\partial z} \ell_y + \frac{\partial \widehat{C}}{\partial y} \ell_z \right) \right] N_i d \Gamma \end{aligned} \tag{25}$$

$$\begin{aligned}
 [B4_{ij}] &= \frac{1}{\Delta t} \sum_e \int_{-1}^1 \int_{-1}^1 \int_{-1}^1 (N_i N_j) |J| d\xi d\eta d\zeta \\
 B4_{ij} &\neq 0 \text{ if } i = j
 \end{aligned}
 \tag{26}$$

Finally Eq. 18 may be written as:

$$[B4_{ij}] + \theta ([B1_{ij}] + [B2_{ij}])\{C_j\}_{t+\Delta t} = [B4_{ij}] - (1 - \theta) ([B1_{ij}] + [B2_{ij}])\{C_j\}_t + \{B3_i\}
 \tag{27}$$

This study showed that the explicit and Crank-Nicolson ($\theta=0$ to 0.5) time marching scheme resulted in a numerical oscillating behavior, global errors and convergence problems for transient groundwater flow and solute transport simulations. The model become stable when time marching scheme was changed from the Crank-Nicolson to the Implicit ($\theta=0.6$ to 1.0). The detailed solution of Eqs. 1 and 2 based on the Galerkin weighted residual method is available (Bear and Cheng (2010); Smith and Griffiths (2004); Thangarajan (2007)).

4 Model Calibration

The model was calibrated against spatial and temporal observations of hydraulic heads measured from observation wells and water salinity at the HTW, NTW, STW and KTW agricultural farms. The objective of the model calibration was to minimize the differences between observed field data and model simulated results in terms of head and concentration at corresponding node points. For model calibration, the well domain was discretized into 1,372 nodes and 1,014 elements to accommodate aquifer characteristics, tube well geometry, observation wells configurations and their locations and the constant boundaries. A total of 364 corner nodes were assigned as constant head boundaries and 508 nodes (bottom and corner of the domain) were assigned to the constant concentration boundaries as shown in Fig. 4. The values of local watertable elevation measured from the observation wells were assigned as initial and constant flow boundaries to solve Eq. 1. Similarly, the values of groundwater concentration measured in the study area (Fig. 3) were used as initial and constant concentration boundaries to solve Eq. 2.

The results of computed and observed heads for transient groundwater flow at the HTW, NTW, STW and KTW agricultural farms were summarized and graphically presented in Fig. 5. The best fit line was drawn using the linear least squares method, to evaluate the discrepancies between the simulated and observed heads. An adjusted R^2 value of 0.9738 suggested that model simulated values and observed values for transient groundwater flow were in good agreement. Figure 6 showed the comparison between the computed and observed well salinity for the selected tube wells. The best fit line (dotted line) drawn using the least squares method with an adjusted R^2 (0.9165) showed that computed well salinity commensurate those of observed well salinity. It can be seen from the Fig. 6 that the model underestimated the well salinity for initial time steps (well salinity values below the 1:1 solid line) and overestimated as pumping time increased (well salinity values above the 1:1 solid line). The aquifer parameters determined during model calibration are shown in Table 2. Several statistical approaches could be found in literature that evaluated the model performances against the field data (Hong et al. 2002; Nash and Sutcliffe 1970; Petalas and

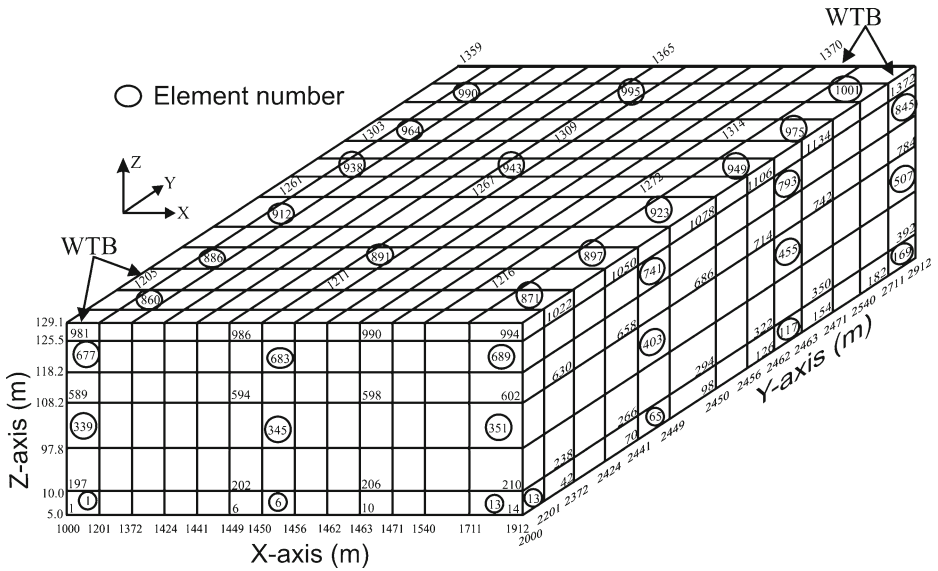


Fig. 4 Discretization of finite element model (not to scale)

Lambrakis 2006; Willmott 1982; Willmott 1981; Yang et al. 2009; Yapo et al. 1996). For this study six statistical indices i.e. adjusted R^2 , mean absolute error (MAE), root mean squared error (RMSE), Nash-Sutcliffe efficiency or model efficiency (ME), BIAS, and index of

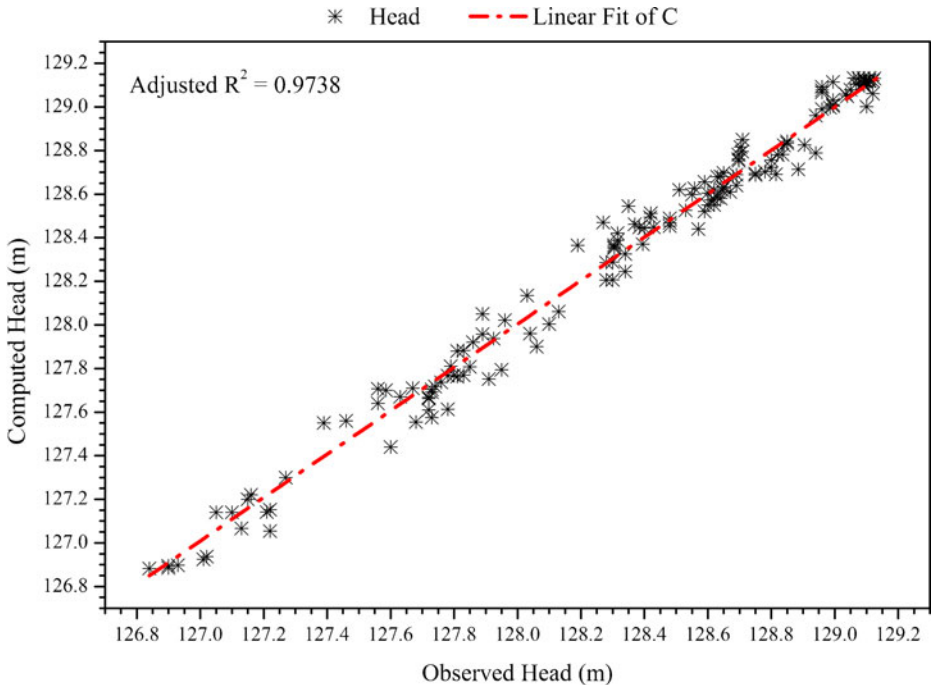


Fig. 5 Scatter plot for observed and simulated head for transient groundwater flow

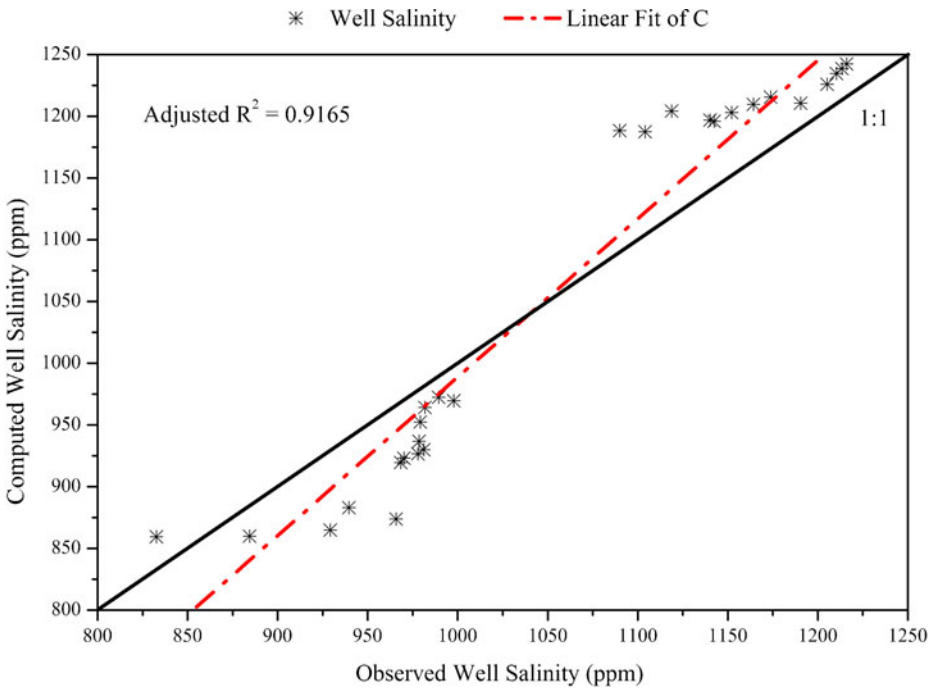


Fig. 6 Scatter plot for observed and simulated well salinity

agreement (d) were employed to evaluate the goodness of the model simulation for saturated groundwater flow and solute transport. The values of these statistical performance indices (Table 3) showed that the overall model performance for groundwater flow and solute transport is good and accurate within generally acceptable tolerances.

Overall, the statistical evaluation of the FEMGWST model suggested that it was a reliable tool for investigating and understanding the response of aquifer system under the existing geo hydro conditions of the Lower Indus Basin, Pakistan. The calibrated model was next used to predict the impacts of different well configurations and variation in pumping rate, pumping time, number of well strainers, horizontal distance between well strainers and

Table 2 Aquifer parameters values of different material obtained by model calibration

Material name	Kx	Ky	Kz	S _S (10 ⁻³)	a _L	a _{T1}	a _{T2}	η
Coarse Sand	28.80	28.80	14.40	1.00	3.50	1	1	0.35
Fine Sand	20.16	20.16	7.20	1.00	3.20	0.8	0.8	0.36
Sandy Loam	3.31	3.31	1.44	0.40	3.00	0.8	0.8	0.36
SILTY LOAM	2.52	2.52	1.26	0.35	2.5	0.8	0.8	0.38
Canal Embankment	0.50	0.50	0.15	0.20	2.00	0.70	0.70	0.40
Impervious	0.18	0.18	0.04	0.10	2.00	0.70	0.70	0.41

K is hydraulic conductivity (m day⁻¹) in x, y and z direction, S_S is specific storage (m⁻¹), a_L is longitudinal dispersivity (m), a_{T1} and a_{T2} are transversal dispersivities (m) and η is porosity

Table 3 Statistical evaluation of FEMGWST model

Model Type	Adjusted R ²	RMSE	MAE	ME	BIAS (10 ⁻³)	d
Steady Flow	0.996	0.040	0.030	0.996	-0.026	0.999
Transient flow	0.974	0.102	0.072	0.973	0.023	0.993
Solute Transport	0.916	48.650	43.548	0.817	1.442	0.966

thickness of fresh-saline water interface on the quality of the pumping water and the development of salinity mound at the bottom of the well.

5 Model Applications

5.1 Impact of Well Discharge and Number of Well Strainers on Water Quality

During field surveys, it was noted that well operation times vary from a few hours to 6 days and the well discharges vary between 15 and 30 l per second (lps). The stress on groundwater supplies is increased during times of irrigation canal closure time and also of the periods of crop sowing. The model was run to assess the impacts of different well discharges i.e. 15, 20, 25 and 30 lps through single, double, triple and quadruple strainers skimming well on the groundwater quality. The strainers in the double, triple and quadruple configurations were spaced 12 m apart from each other. The temporal increase in the quality of pumping water for different well discharges flowing through single, double, triple and quadruple strainers skimming well is illustrated in Fig. 7. The simulated values of the well salinity for the different well discharges through single and multi strainers wells are summarized in Tables 4 and 5 for the pumping time of 3 and 180 h respectively. The simulated values of well salinity through a single strainer well were 1187.53, 1189.34, 1185.42 and 1185.66 ppm for the well discharges of 15, 20, 25 and 30 lps respectively for a pumping time of 3 h. The water salinity of quadruple strainers well was reduced to 1176.42, 1182.10, 1182.10 and 1180.83 ppm respectively for the corresponding well discharges after an operation time of 3 h. The maximum absolute difference due to well discharges was noted at 6.42 ppm. Similarly, the maximum absolute difference due to the number of well strainers was recorded to be 11.52 ppm. Differences in the well salinity increased with pumping time. For example at the pumping time of 180 h the maximum absolute difference in the pumping water salinity was 73.00 ppm for the given well discharges and 40.44 ppm due to numbers of well strainers (Table 5). It can be seen from the results in Tables 4 and 5 that there was minimum difference in the quality of the pumping water obtained through triple and quadruple strainers skimming wells.

5.2 Impact of Thickness of Fresh-Saline Water Interface on Water Quality

The designs of existing farmers' tubewells installed in the study area were not based on any site specific knowledge of aquifer characteristics and groundwater salinity profile.

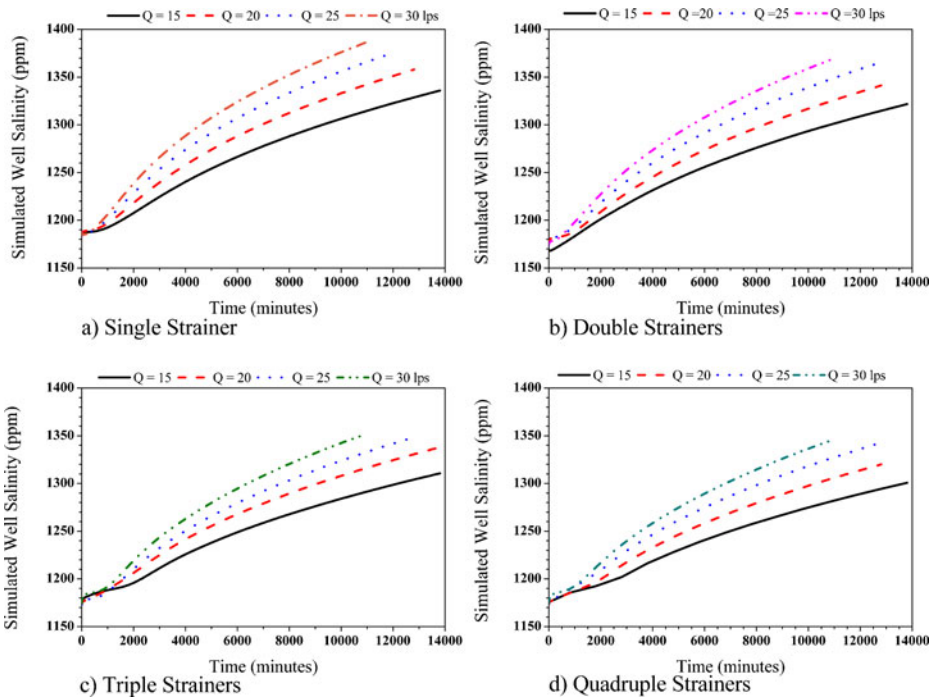


Fig. 7 Impact of different well discharges on the quality of the pumping water through single and multi strainer wells

It is also a known fact that farmers in the area did not take care about the thickness of fresh-saline water interface (TFS). Hence many wells were abandoned as a result of the poor quality of the pumping water. FEMGWST model was run to assess the impacts of different thicknesses of the fresh-saline water interface (4, 7 and 10 m) on the quality of the pumped water through single and multi strainer(s) skimming wells for pumping discharge rates of 20 and 30 lps. Figure 8a revealed that the quality of water through double strainers well increased with decrease in the thickness of fresh-saline water interface and should rightly be so.

It was observed that the simulated well salinity flowing at the rate of 20 lps were 1224.66, 1241.41 and 1271.24 ppm respectively for the 10, 7 and 4 m thickness of fresh-saline water interfaces, at a pumping duration of 30 h. The well salinity was increased to 1333.98, 1349.46 and 1379.83 ppm after a pumping time of 160 h for the same given fresh-saline water interfaces. The difference in the pumping water salinity was 15 and 31 ppm for the thickness of fresh-saline water interface decreasing from 10 to 7 m and from 7 to 4 m respectively. The same trend is observed for the well discharge of 30 lps. Similarly, pumping water salinity trends for the given values of well discharges and fresh-saline water interface thicknesses through single, double, triple and quadruple strainers well were almost the same.

Table 4 Salinity of the pumping water as affected by the well discharges and number of strainers (T=3 h; TFS=10 m)

Number of Strainers	Salinity Q1 (ppm)	Salinity Q2 (ppm)	Salinity Q3 (ppm)	Salinity Q4 (ppm)
S1	1187.53	1189.34	1185.42	1185.66
S2	1181.20	1177.82	1178.90	1184.50
S3	1177.82	1177.60	1178.60	1184.24
S4	1176.42	1182.10	1182.10	1180.83
Difference in salinity due to well discharge				
	Salinity (Q1-Q2)	Salinity (Q1-Q2)	Salinity (Q1-Q2)	Salinity (Q1-Q2)
S1	1.81	-3.91	0.24	-1.87
S2	-3.38	1.08	5.60	3.30
S3	-0.21	1.00	5.64	6.42
S4	5.68	0.00	-1.27	4.41
Difference in salinity due to well strainers				
	Salinity Q1	Salinity Q2	Salinity Q3	Salinity Q4
Salinity (S1-S2)	6.33	11.52	6.52	1.16
Salinity (S2-S3)	3.38	0.21	0.30	0.26
Salinity (S3-S4)	1.40	-4.50	-3.50	3.41
Salinity (S1-S4)	11.11	7.24	3.32	4.83

Q are well discharges (Q1 = 15, Q2 = 20, Q3 25 and Q4 = 30 lps), S is number of Strainer (S1 = single, S2 = Double, S3 = Triple and S4 = Quadruple strainers well), T is Time and TFS is thickness of fresh saline water interface

Table 5 Salinity of the pumping water as affected by well discharges and number of strainers (T=180 h; TFS=10 m)

Number of Strainers	Salinity Q1 (ppm)	Salinity Q2 (ppm)	Salinity Q3 (ppm)	Salinity Q4 (ppm)
S1	1313.23	1340.70	1364.27	1386.23
S2	1299.94	1324.35	1347.37	1369.13
S3	1290.18	1314.89	1331.42	1351.71
S4	1280.68	1304.44	1325.88	1345.79
Difference in salinity due to well discharge				
	Salinity (Q1-Q2)	Salinity (Q1-Q2)	Salinity (Q1-Q2)	Salinity (Q1-Q2)
S1	27.47	23.57	21.96	73.00
S2	24.42	23.02	21.76	69.20
S3	24.70	16.53	20.30	61.53
S4	23.76	21.45	19.91	65.12
Difference in salinity due to well strainers				
	Salinity Q1	Salinity Q2	Salinity Q3	Salinity Q4
Salinity (S1-S2)	13.29	16.34	16.90	17.10
Salinity (S2-S3)	9.75	9.47	15.96	17.42
Salinity (S3-S4)	9.51	10.45	5.53	5.92
Salinity (S1-S4)	32.55	36.26	38.39	40.44

Notations are defined in Table 4

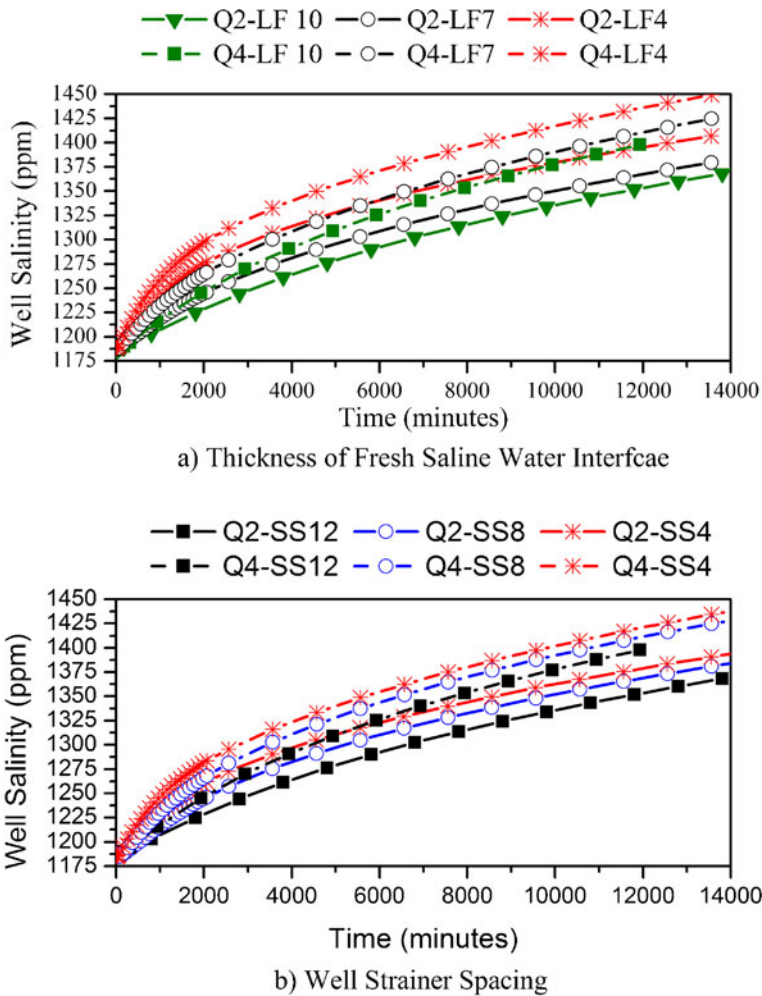


Fig. 8 Well salinity for different thicknesses fresh saline water interfaces and well strainer spacing

5.3 Impact of Well Strainer Spacing on Pumping Water Quality

The choice of horizontal distance between the strainers in pumping well is based on the hydrogeology of the site, pumping conditions, and the allowance provided for the drawdown to overlap. The impact of distance between the strainers of a well (4, 8 and 12 m) on the quality of pumping water was simulated for double strainers skimming well flowing at the rate of 20 and at 30 lps. The fresh-saline water interface thickness was kept to 10 m. Figure 8b shows the impacts of the strainer spacing on the quality of double strainers well flowing at the rate of 20 and at 30 lps. It is depicted in Fig. 8b that the difference in the pumping water quality due to variation in strainer spacing is less than 10 ppm after a well operation time of 3 h and this difference increased to 25 ppm after a pumping duration of 30 h and thereafter simulated groundwater quality lines are almost parallel to each other for the strainer spacings of 4, 8 and 12 m.

Saeed and Bruen (2004) pointed out the spatial distance between the bore holes has almost no effect on the pumped water salinity. However, this study suggested that the strainer spaced 12 m apart from each other (represented through solid lines) offer better alternative to control the pumping water salinity. It is also a fact that the material, operational and maintenance costs of the pumping well is increased with the increase in the number of strainers and the distance between them and this has to be considered.

5.4 Saline Water Intrusion at the Bottom of the Well

The FEMGWST model was also used to investigate the impacts of different well pumping rates and well configurations on the groundwater salinity at the bottom of the single and multi strainer (s) skimming wells. Although the variation in the quality of the pumping water is quite obvious and farmer may be aware of it, however the mechanism of the groundwater quality deterioration beneath the ground surface is unknown to him. Thus, the changes in the groundwater salinity for different well discharges at the bottom of skimming well were simulated. The length of the blind pipe was kept a 10 m, the well strainer length was 12.0 m, the thickness of fresh-saline water interface was kept to 10.0 m, the initial salinity value assigned at the bottom of the well was 1,190 ppm and the domain area consists of 83.17 ha, as designed for the HTW (Fig. 4).

5.4.1 Maximum Groundwater Salinity for Different Well Configurations

Results showed that groundwater salinity moved in the shape of a growing mound towards the bottom of the well(s) so that its apex was at or directly below the bottom of the pumping well. The values of the maximum simulated salinity at the base of the skimming well for the different well configurations are summarized in Table 6 for the pumping times of 12, 30 and

Table 6 Intermittent pumping effects on peak of salinity mound development at the bottom of the well

	T=12 hr	T=30 hr	T=144 hr	(30–12)hr	(144–30)hr	(144–12)hr
	Maximum salinity (ppm) at the bottom of the well			Difference in Maximum salinity (ppm)		
Q1-S1	1259.05	1300.43	1389.92	41.38	89.49	130.87
Q1-S2	1252.62	1293.89	1385.28	41.27	91.39	132.66
Q1-S3	1241.62	1282.43	1379.63	40.81	97.20	138.01
Q1-S4	1233.31	1273.28	1379.00	39.97	105.72	145.69
Q2-S1	1272.75	1315.71	1406.72	42.96	91.01	133.97
Q2-S2	1265.84	1312.00	1401.65	46.16	89.65	135.81
Q2-S3	1254.54	1298.75	1397.75	44.21	99.00	143.21
Q2-S4	1244.65	1289.51	1396.90	44.86	107.39	152.25
Q3-S1	1284.36	1327.77	1421.08	43.41	93.31	136.72
Q3-S2	1277.26	1321.74	1415.85	44.48	94.11	138.59
Q3-S3	1265.50	1311.64	1410.85	46.14	99.21	145.35
Q3-S4	1255.39	1303.36	1411.98	47.97	108.62	156.59
Q4-S1	1293.82	1339.77	1431.08	45.95	91.31	137.26
Q4-S2	1286.88	1335.89	1429.30	49.01	93.41	142.42
Q4-S3	1275.44	1322.44	1423.27	47.00	100.83	147.83
Q4-S4	1264.80	1319.94	1422.16	55.14	102.22	157.36

Notations are defined in Table 4

180 h. Table 6 shows that the maximum groundwater salinity at the bottom of the single strainer well reached 1259.1, 1272.8, 1284.4 and 1293.8 ppm for the discharges of 15, 20, 25 and 30 lps respectively. The variation in the maximum salinity in response to the incremental well discharge of 5 lps ranged between 9.45 and 13.70 ppm for the pumping time of 12 h. However the difference in the maximum salinity was 34.77 ppm when well discharge changed from 15 to 30 lps. It can be seen from Table 6 that the rises in groundwater salinity almost follow the same trend for double, triple and quadruple strainers well for the given discharges. However, the mechanism of groundwater quality degradation is intensified rapidly with the pumping time.

5.4.2 Horizontal Groundwater Salinity Distribution for Different Well Configurations

The horizontal distribution of groundwater salinity (higher than 1,200 ppm) for the given well discharges and the number of well strainers at the pumping time of 12, 30 and 144 h are summarized into Tables 7 and 8. The groundwater deteriorating process is measured in terms of area in hectares and percentage of the total area. The most striking result to emerge from the data is that the well discharges and the pumping time are the key players to suppress the saline water intrusion process as compared to the number of well strainers. It was observed that the variation in the affected area ranged from 3.3 to 9.2 ha, 30.16 to 38.95 ha and 33.5 to 47.29 ha for the pumping period of 30 and 12 h; 144 and 30 h; and 144 and 12 h respectively, for the corresponding well configurations. It was further observed that the maximum horizontal spreading of saline plumes containing salinity greater than 1,200 ppm

Table 7 Horizontal groundwater salinity distribution (>1,200 ppm) in ha at the bottom of the well for different thicknesses of fresh saline water interfaces (TFS)

Category	Pumping Time=12 hr			Pumping Time=30 hr			Pumping Time=144 hr		
	TFS4	TFS7	TFS10	TFS4	TFS7	TFS10	TFS4	TFS7	TFS10
Q1-S1	2.77	1.35	1.32	15.47	7.51	4.35	52.77	41.46	34.92
Q1-S2	3.16	1.55	1.14	15.42	7.69	4.64	52.73	41.34	34.80
Q1-S3	2.96	1.44	1.02	15.41	7.55	4.46	52.74	41.36	34.79
Q1-S4	2.90	1.50	1.06	15.32	7.45	4.40	52.77	41.44	34.87
Q2-S1	4.98	2.18	1.57	19.83	10.86	6.64	57.72	47.83	41.06
Q2-S2	4.95	2.47	1.80	19.62	10.81	6.84	57.68	47.75	40.96
Q2-S3	4.68	2.32	1.68	19.68	10.75	6.72	57.69	47.75	40.95
Q2-S4	4.48	2.33	1.69	19.69	10.66	6.66	57.71	47.81	41.02
Q3-S1	6.44	3.11	2.22	24.40	13.69	8.91	61.24	52.43	46.23
Q3-S2	6.77	3.46	2.48	24.16	13.62	8.97	61.21	52.40	46.15
Q3-S3	6.63	3.29	2.34	24.34	13.62	8.86	61.23	52.39	46.13
Q3-S4	6.34	3.24	2.35	24.31	13.60	8.87	61.24	52.43	46.20
Q4-S1	8.32	4.06	2.91	28.36	16.62	8.91	63.87	55.79	50.04
Q4-S2	8.48	4.36	3.17	28.12	16.39	12.21	63.84	55.74	50.33
Q4-S3	8.32	4.18	3.04	28.22	16.43	11.09	63.85	55.77	50.04
Q4-S4	8.16	4.09	3.00	28.29	16.48	12.19	63.86	55.77	50.36

TFS is Thickness of fresh saline water interface, 4, 7 and 10 is the thickness in m; remaining parameters were described in previous tables

Table 8 Affected area in percentage with groundwater salinity higher than 1,200 ppm at the bottom of the well for different thicknesses of fresh saline water interfaces (TFS)

Category	Pumping Time=12 hr			Pumping Time=30 hr			Pumping Time=144 hr		
	TFS4	TFS7	TFS10	TFS4	TFS7	TFS10	TFS4	TFS7	TFS10
Q1-S1	3.33%	1.63%	1.59%	18.60%	9.03%	5.23%	63.45%	49.85%	41.98%
Q1-S2	3.80%	1.87%	1.38%	18.53%	9.25%	5.58%	63.39%	49.71%	41.84%
Q1-S3	3.56%	1.73%	1.22%	18.53%	9.08%	5.36%	63.40%	49.73%	41.83%
Q1-S4	3.49%	1.80%	1.28%	18.42%	8.95%	5.28%	63.45%	49.83%	41.93%
Q2-S1	5.99%	2.62%	1.89%	23.84%	13.05%	7.98%	69.39%	57.51%	49.37%
Q2-S2	5.95%	2.97%	2.16%	23.59%	12.99%	8.23%	69.35%	57.41%	49.24%
Q2-S3	5.62%	2.79%	2.02%	23.66%	12.92%	8.08%	69.36%	57.41%	49.24%
Q2-S4	5.39%	2.80%	2.03%	23.67%	12.82%	8.00%	69.39%	57.48%	49.32%
Q3-S1	7.74%	3.74%	2.67%	29.34%	16.46%	10.72%	73.63%	63.04%	55.58%
Q3-S2	8.14%	4.16%	2.98%	29.05%	16.37%	10.78%	73.60%	63.00%	55.49%
Q3-S3	7.97%	3.95%	2.81%	29.26%	16.37%	10.66%	73.61%	62.98%	55.46%
Q3-S4	7.62%	3.90%	2.82%	29.23%	16.36%	10.67%	73.63%	63.04%	55.54%
Q4-S1	10.00%	4.88%	3.49%	34.09%	19.98%	10.72%	76.79%	67.07%	60.16%
Q4-S2	10.19%	5.25%	3.81%	33.81%	19.71%	14.69%	76.75%	67.02%	60.51%
Q4-S3	10.00%	5.02%	3.66%	33.93%	19.75%	13.33%	76.76%	67.05%	60.16%
Q4-S4	9.81%	4.92%	3.61%	34.01%	19.82%	14.66%	76.78%	67.05%	60.55%

All parameters were described in previous tables

is about 3.8, 14.8 and 60.6% of the total area for the pumping times of 12, 30 and 144 h, respectively for the given well configurations.

5.4.3 Horizontal Groundwater Salinity Distribution for Different Thicknesses of Fresh-Saline Water Interfaces

In previous sections, the impacts of different hydrological conditions (well discharges, the number of well strainers and the well operation time) for a constant 10 m thickness of fresh-saline water interface on the saline water intrusion were evaluated. In this section the relation among the different thicknesses of fresh-saline water interface and saline water intrusion is described. The results of each hydrological condition for different thicknesses of the fresh-saline water interface (4, 7 and 10 m) in terms of the maximum groundwater salinity are shown in Fig. 9 and the area with groundwater salinity higher than 1,200 ppm at the bottom of the pumping well are summarized in Tables 7 and 8. Each part of Fig. 9 summarizes the combination of 36 different scenarios for the given well discharge.

Figure 9a reveals that the maximum simulated groundwater salinity at the bottom of the single strainer well is 1312.5, 1277.15 and 1259.05 ppm for the fresh-saline water interface thickness of 4, 7 and 10 m respectively for the pumping rate of 15 lps through single strainer at a pumping duration of 12 h. It was observed that the difference in the maximum salinity is 35.35, 18.1 and 53.45 ppm due to varying the fresh-saline water interface thickness from 4 to 7, 7 to 10 and 4 to 10 m, respectively. Figure 9 depicts that maximum salinity is directly

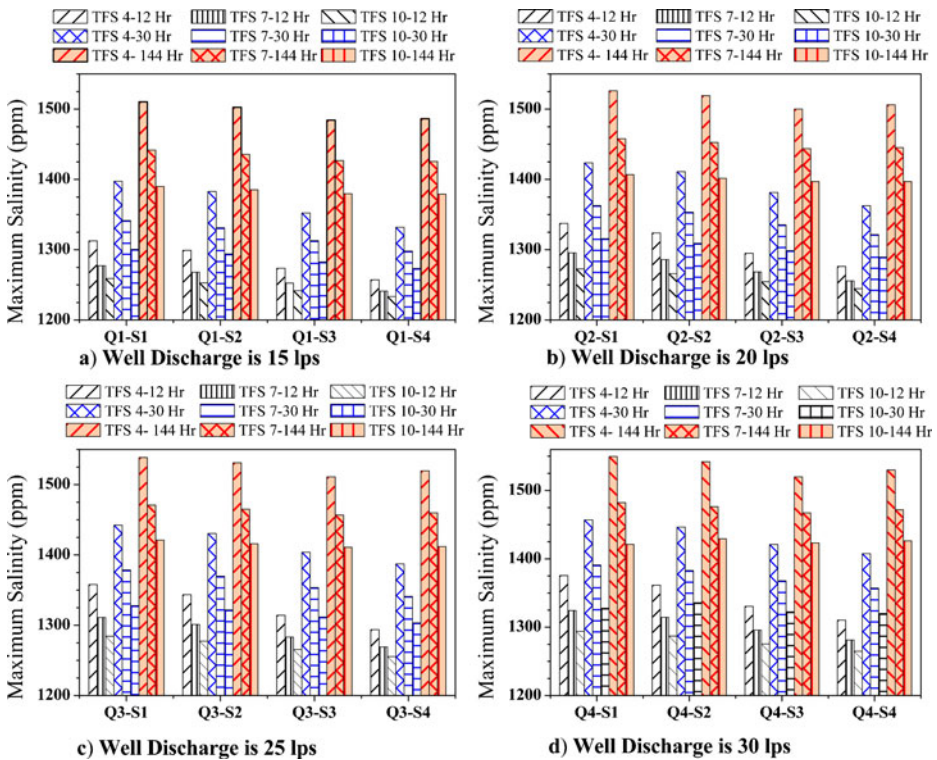


Fig. 9 Values of saline plume peak at the bottom of the well for various well configurations

related to well discharge, well operation time and inversely to the thickness of fresh-saline water interface and the number of well strainers. For example when the fresh-saline water interface thickness decreased from 10 to 4 m, the maximum salinity increased from 1300.43 to 1397.82, and from 1389.92 to 1510.26 ppm at the pumping duration of 30 and 144 h and the difference in maximum salinity increased to 97.39 and 120.34 ppm for single strainer well. Figure 9 also illustrated that as the pumping time was increased and fresh-saline water interface thickness decreased, the effects of multi strainers well to minimize the saline water intrusion were decreased. For example the variation in the difference of the maximum salinity among single and quadruple strainers well is 29.63 ppm, for the fresh-saline water interface decreased from 10 to 4 m at the pumping duration of 12 h and 12.93 ppm at the pumping duration of 144 h.

From the model results it was found that the multi strainer wells could effectively suppress the development of the salinity mound compare to single strainer wells. However, when the thickness of the fresh-saline water interface reduces to 4 m then the quadruple strainer wells could induce the saline water intrusion. A possible explanation of this observation is that as the fresh-saline water interference decreases to 4 m, the apex of plumes intercepted by the well strainers and salt plume started spreading horizontally as pointed out by Werner et al. (2009).

The horizontal distribution of groundwater salinity at the bottom of the well was also evaluated for the given thicknesses of fresh-saline water interface. Table 7 showed that 1.32,

1.35 and 2.77 ha contained groundwater salinity higher than 1,200 ppm for the fresh-saline water interface thickness of 4, 7 and 10 m respectively at a pumping rate of 15 lps through single strainer for a pumping duration of 12 h. However the multi strainers well offered better alternative to control the saline water intrusion. The contaminated area decreased to 1.06, 1.50 and 2.90 ha for the same given conditions with quadruple strainer well. Table 7 further revealed that the area containing groundwater salinity higher than 1,200 ppm was 1.32, 4.35 and 34.92 ha for the single strainer well after an operation time of 12, 30 and 144 h respectively, for the fresh-saline water interface of 10 m. The contaminated area increased to 1.35, 7.51 and 41.46 ha for the fresh-saline water interface of 7 m and affected area further increased to 2.76, 15.47 and 52.77 ha when the fresh-saline water interface decreased to 4 m respectively for the given pumping durations. Table 8 showed the contaminated area in percentage and it can be seen that the affected area is about 1.59, 1.63 and 3.33% of the total domain area for the saline water interface 10, 7 and 4 m respectively for the pumping duration of 12 h and the said area is increased to 5.23, 9.03 and 18.60; and 41.98, 49.85 and 63.45% for the pumping duration of 30 and 144 h respectively. As the number of well strainer increased, the horizontal distribution of groundwater salinity is slightly changed and maximum absolute difference in the area contained groundwater salinity higher than 1,200 ppm is around 0.26 ha (Table 7).

The horizontal spreading of salinity plume under a single strainer well continued with the pumping time and when pumping duration increased from 12 to 144 h the affected area increased from 1.32 ha to 34.92 ha for the well discharge of 15 lps. The affected area was further increased to 50.04 ha when well pumping rate increased to 30 lps with the fresh-saline water interface thickness of 10 m. when the fresh-saline water interface decreased 7 and 4 m the corresponding change in the area is 55.79 and 63.87 ha respectively.

6 Conclusions

A three dimensional finite element model for groundwater flow and solute transport (FEMGWST model) was developed and calibrated with field data. The values of six statistical indices (Adjusted R^2 , mean absolute error, root mean squared error, Nash-Sutcliffe efficiency or model efficiency, BIAS, and index of agreement) showed that the overall model performance for groundwater flow and solute transport simulations showed good agreement with the corresponding observed field data. The model became stable when the time marching scheme was changed from the Crank-Nicolson to the Implicit (Theta=0.6 to 1.0).

The calibrated model was used to analyze the possible changes to the pumped water quality and the behavior of the mechanism of saline water intrusion at the bottom of the pumping well in response to different well configurations and pumping parameters. It was observed that groundwater salinity envelope moved in the shape of a growing mound towards the bottom of the well(s) so that its apex was at or directly below the bottom of the pumping well.

A curvilinear relationship was established between pumping duration and quality of pumping water for the well discharges of 15, 20, 25 and 30 lps through single, double, triple or quadruple strainer(s) skimming wells. The impacts of the thickness of the fresh-saline water interface (TFS) i.e. 4, 7 and 10 m on well salinity was also evaluated. Results showed that the groundwater salinity increased with decrease in the thickness of fresh-saline water interface as would be expected. In general it was concluded that the performance of the multi strainers skimming well was better than the single strainer skimming well as far as pumping water quality is of concern. However when the fresh-saline water interface

thickness decreased to 4 m, the quadruple strainers well accelerated the saline water intrusion into the fresh groundwater instead of suppressing it because the apex of the saline plumes intercepted by the base of the well strainers and saline mound started spreading horizontally. The impacts of spacing between strainers in wells (2, 4, 8 and 12 m) on the quality of pumping water was only studied with double and quadruple strainer wells flowing at the rates of 20 and 30 lps. It was observed that the variation in the strainer spacing was not a prominent factor to suppress the saline water intrusion.

Overall it is concluded that the groundwater quality is proportional to well discharges, pumping duration and inversely proportional to the thickness of fresh-saline water interface, the number of well strainers and the horizontal distance between the well strainers.

Acknowledgements The development of FEMGWST model and numerical evaluation of this research was carried out at Universiti Pura Malaysia, Malaysia. The authors are grateful to the farmers of the project area and Drainage and Reclamation Institute of Pakistan (DRIP) for their cooperation in conducting the field experiments.

References

- Ahmad Z, Ashraf A, Fryar A, Akhter G (2010) Composite use of numerical groundwater flow modeling and geoinformatics techniques for monitoring Indus Basin aquifer, Pakistan. *Environ Monit Assess* (173) 447–457. doi:10.1007/s10661-010-1398-3
- Ataie-Ashtiani B, Ketabchi H (2010) Elitist continuous ant colony optimization algorithm for optimal management of coastal aquifers. *Water Resour Manag* 25(1):165–190. doi:10.1007/s11269-010-9693-x
- Bear J, Cheng AH-D (2010) Modeling groundwater flow and contaminant transport. Springer, Dordrecht, Heidelberg, London, New York
- Bear J, Verruijt A (1990) Modeling of groundwater flow and pollution. D. Reidel Pub. Co, Dordrecht
- Chandio BA, Larock BE (1984) Three-dimensional model of a skimming well. *J Irrig Drain Eng* 110:275–288. doi:10.1061/(ASCE)0733-9437(1984)110:3(275)
- Hong Y, Rosen MR, Reeves RR (2002) Dynamic fuzzy modeling of storm water infiltration in urban fractured aquifers. *J Hydrol Eng* 7(5):380–391
- Iglesias A, Garrote L, Flores F, Moneo M (2007) Challenges to manage the risk of water scarcity and climate change in the Mediterranean. *Water Resour Manag* 21:775–788. doi:10.1007/s11269-006-9111-6
- Khan S, Rana T, Gabriel HF, Ullah MK (2008) Hydrogeologic assessment of escalating groundwater exploitation in the Indus Basin, Pakistan. *Hydrogeol J* 16:1635–1654
- Kourakos G, Mantoglou A (2010) Simulation and multi-objective management of coastal aquifers in semi-arid regions. *Water Resour Manag* 25(4):1063–1074. doi:10.1007/s11269-010-9677-x
- Lenkopane MK, Werner AD, Lockington DA, Li L (2009) Influence of variable salinity conditions in a tidal creek on riparian groundwater flow and salinity dynamics. *J Hydrol* 375:536–545. doi:10.1016/j.jhydrol.2009.07.004
- Nash JE, Sutcliffe JV (1970) River flow forecasting through conceptual models. Part I—a discussion of principles. *J Hydrol* 10:282–290
- Pakistan Agricultural Machinery Census (2004) Government of Pakistan, statistics division, agricultural census organization. <http://www.statpak.gov.pk/depts/aco/publications/agricultural-machinery-census2004/amc2004.html>
- Pakistan Water Economy Running Dry (2005) Published by World Bank Call Number: ARD 2005
- Hunting Technical Services Ltd and Macdonald & Partners (1965) Lower Indus report, water and power development authority, Volume 6
- Petalas C, Lambrakis N (2006) Simulation of intense salinization phenomena in coastal aquifers—the case of the coastal aquifers of Thrace. *J Hydrol* 324:51–64
- Qureshi AS, McCornick PG, Qadir M, Aslam Z (2008) Managing salinity and waterlogging in the Indus Basin of Pakistan. *Agric Water Manag* 95:1–10
- Qureshi AS, McCornick PG, Sarwar A, Sharma BR (2010) Challenges and prospects of sustainable groundwater management in the Indus Basin, Pakistan. *Water Resour Manag* 24:1551–1569
- Rejani R, Madan KJha, Panda SN, Mull R (2008) Simulation modeling for efficient groundwater management in Balasore Coastal Basin, India. *Water Resour Manag* 22:23–50. doi:10.1007/s11269-006-9142-z

- Saeed MM, Ashraf M (2005) Feasible design and operational guidelines for skimming wells in the Indus Basin, Pakistan. *Agri Water Manag* 74:165–188
- Saeed MM, Bruen M (2004) Simulation of hydrosalinity behavior under skimming wells. *Irrig Drain Syst* 18:1–34
- Smith IM, Griffiths DV (2004) Programming the finite element method (4th ed). John Wiley & Sons, Ltd. The Atrium, southern gate, Chichester, west Sussex PO19 8SQ, England
- Sufi AB, Latif M, Skogerboe GV (1998) Simulating skimming well techniques for sustainable exploitation of groundwater. *Irrig Drain Syst* 12:203–226
- Thangarajan M (2007) Groundwater flow and mass transport modeling: theory and applications. Capital publishing company, New Delhi
- Werner AD, Jakovovic D, Simmons CT (2009) Experimental observations of saltwater up-coning. *J Hydrol* 373:230–241
- Willmott CJ (1981) On the validation of model. *Phys Geogr* 2:183–194
- Willmott CJ (1982) Some comments on the evaluation of model performance. *Bull Amer Meteorol Soc* 63:1309–1369. doi:10.1175/1520-0477(1982)063<1309:SCOTEO>2.0.CO;2
- Yang ZP, Lu WX, Long YQ, Li P (2009) Application and comparison of two prediction models for groundwater levels: a case study in Western Jilin Province, China. *J Arid Environ* 73:487–492
- Yapo PO, Gupta HV, Sorooshian S (1996) Automatic calibration of conceptual rainfall-runoff models: sensitivity to calibration data. *J Hydrol* 181:23–48
- Yu FX (1992) Modeling three-dimensional groundwater flow and solute transport by the finite element method with parameter estimation. Doctoral Dissertation. The Louisiana State University and Agricultural and Mechanical College
- Zardari N, Cordery I (2009) Water productivity in a rigid irrigation delivery system. *Water Resour Manag* 23:1025–1040. doi:10.1007/s11269-008-9312-2